New Internal Structure of Spider Dragline Silk Revealed by Atomic Force Microscopy

S. F. Y. Li, A. J. McGhie, and S. L. Tang
DuPont Central Research and Development, Experimental Station, Wilmington, Delaware 19880–0356 USA

ABSTRACT Atomic force microscopy was used to study the three-dimensional nanometer-scale structure of the dragline silk of *Nephila clavipes* from microtomed sections of the silk. Contrary to a previously proposed model of randomly distributed protein crystallites interspersed in amorphous regions, a highly organized skin-core structure of the fiber was observed. The skin appeared to be thin with no discernible distinct features. The core consists of pleated fibril-like structures, which are arranged in two concentric cylinders. Upon stretching, the pleats were smoothed out substantially. The mechanical properties of spider silk can quite straightforwardly be related to the newly observed structures.

INTRODUCTION

The mechanical properties of spider dragline silk shows a unique combination of high modulus, high tensile strength, and high elasticity (Gosline et al., 1986; Denny, 1986), which has not been reproduced in synthetic fibers. Moreover, because of its protein composition, spider silk is biodegradable and hence is an environmentally desirable alternative to nonbiological polymeric materials. For these reasons, it has attracted much attention for its potential applications as a high-performance fiber (Vollrath, 1992; Beard, 1992). Knowledge of the structure of the silk is critical for understanding the formation and processing of such materials.

The molecular and structural bases for the remarkable properties of spider dragline silk are at present not well understood. Based on structural information of the protein molecules derived from x-ray studies and the hypothesis that the dragline silk is similar to the silk of the silk worm, a structural model for dragline silk has been proposed (Gosline et al., 1986). The silk is believed to be a composite material made of discrete, ordered crystals of antiparallel beta sheets interspersed in regions of disordered amino acid alpha helical chains (Gosline et al., 1986; Vollrath, 1992; Hepburn et al., 1979). Both the crystalline and amorphous regions are commonly believed to be composed of a single protein, fibroin, although recent results suggest the presence of two different proteins (Lewis, 1992).

Several mechanisms have been proposed to account for the elasticity of spider silk with this type of structure. Using Fourier transform infrared spectroscopy, Dong et al. (1991) proposed that either helix formation or reorientation of preexisting helices interspersed among the stable beta-sheet domains takes place when axial tension is applied to the silk fiber. For wetted silk that has supercontracted, Gosline et al. (1984) suggested that the molecular mechanism for the elasticity of spider silk may be attributed to an entropy-driven process similar to that observed in rubber that was based on a non-Gaussian rubber network theory (Treloar, 1975). The plasticizing and surface tension effects of water on the silk (Vollrath and Edmonds, 1989; Edmonds and Vollrath, 1992; Bonthrone et al., 1992; Vollrath et al., 1990; Sanders, 1993) are believed to cause the exceptionally high elasticity of the capture threads of *Araneus diadematus*. To date, neither the structural model nor its relation to the mechanisms for stretching the spider silk have been confirmed. Likewise the question of how the proposed structure could lead to high tensile strength of the silk fiber has not been thoroughly investigated.

High resolution microscopies, obvious choices for deciphering structure-property relationships, have contributed conspicuously little toward understanding the structure-property relationship of spider silk. Transmission electron microscopy has been applied to study the internal structure of the egg case silks of several species of spiders. Fibrils randomly distributed in a matrix within the fiber are suggested in the egg case silk of *A. aurantia* (Stubbs et al., 1992). The cylindrical gland silk fibers of *P. producta* seem to exhibit, at least occasionally, longitudinal bands along the fiber axis, whereas those of *U. walckenaerius* show spheres in a matrix (Peters and Kovoor, 1989). This information is too sketchy to relate to the mechanical properties of the egg case silks. So far no meaningful electron microscopy result has been reported on the dragline silk. The protein composition of the silk may make it difficult for detailed studies with techniques that require high energy electrons.

METHODS AND MATERIALS

We report here the use of the nondestructive, three-dimensional, real space imaging capability of the atomic force microscope (AFM) (Binnig et al. 1986; Hansma et al., 1992; Rammacher et al., 1992) to obtain the internal structure of spider dragline silk. Although the AFM is most widely used for discerning surface structures, for strong fibers such as spider silk the nanometer-scale internal structure of the silk can be determined from images

Received for publication 27 September 1993 and in final form 24 January 1994.

Address reprint requests to Sau Lan Tang, DuPont Central Research and Development, Experimental Station, P.O. Box 80356, Wilmington, DE 19880–0356 USA.

S. F. Y. Li's permanent address is Chemistry Department, National University of Singapore, Singapore.

© 1994 by the Biophysical Society

0006-3495/94/04/1209/04 $2.00

of longitudinal sections and sections made at 45° and 90° to the longitudinal axis of the silk fiber. In addition, the relationship between structural characteristics and the elastic property of the silk was investigated in images of sections of stretched silk fibers.

The force microscope used was a Nanoscope II AFM (Digital Instruments, Goleta, CA). The tips used were microfabricated Ultralevers (Park Scientific Sunnyvale, CA), with a force constant of 0.03 N/m. For all the images presented here, imaging forces were in the range between 3 and 10 nN. We have not observed the commonly reported damage or deformation of biological samples by the AFM tip (Yang and Shao, 1993) during scanning probably because of the unusual toughness of the silk (Gosline et al, 1986). Imaging was performed in the constant force mode. No additional information was obtained with the constant height mode of imaging. The popular method of imaging biological materials under water or other liquids was not attempted because of the known effect of "supercontraction" (Work, 1985) of the silk caused by the absorption of water and of possible unknown effects on the silk that other liquids might have caused. As explained below, caution had to be taken to ensure that the samples were completely dry. The images presented are raw images which have not been subjected to any filtering during or after data acquisition.

The spider silk used was secreted by the major ampullate gland of *Nephila clavipes*. Unstretched silk strands were embedded directly in epoxy, cryomicrotomed at −90°C, and deposited onto freshly cleaved highly oriented pyrolytic graphite or mica for imaging. For the preparation of stretched samples, small lengths of the silk fibers were stretched manually to approximately 20% elongation, glued securely at both ends before being embedded in epoxy, and microtomed in the same manner as the unstretched samples. Images obtained on both graphite and mica exhibited similar features. No identifiable artifacts due to sectioning were observed in any of the images obtained, although rupturing of the fiber because of microtoming at 45° and 90° was observed occasionally. The microtomed surface of the epoxy bore distinct knife marks because of the microtoming and, therefore, could be clearly distinguished from that of the spider silk. In the images presented below, the knife marks in the epoxy background may not show up in the grayscale representation of the images because their relief (<10 nm) was in general much smaller than the silk features. All sections were dried in a vacuum before imaging because of the tendency of the silk to absorb water and expand. Images obtained on samples deposited directly onto the substrate after microtoming without floating the sections in a water trough first exhibited similar features to those dried in a vacuum. Both the cryomicrotoming and the drying of the sections were necessary sample preparation steps for obtaining the images shown below.

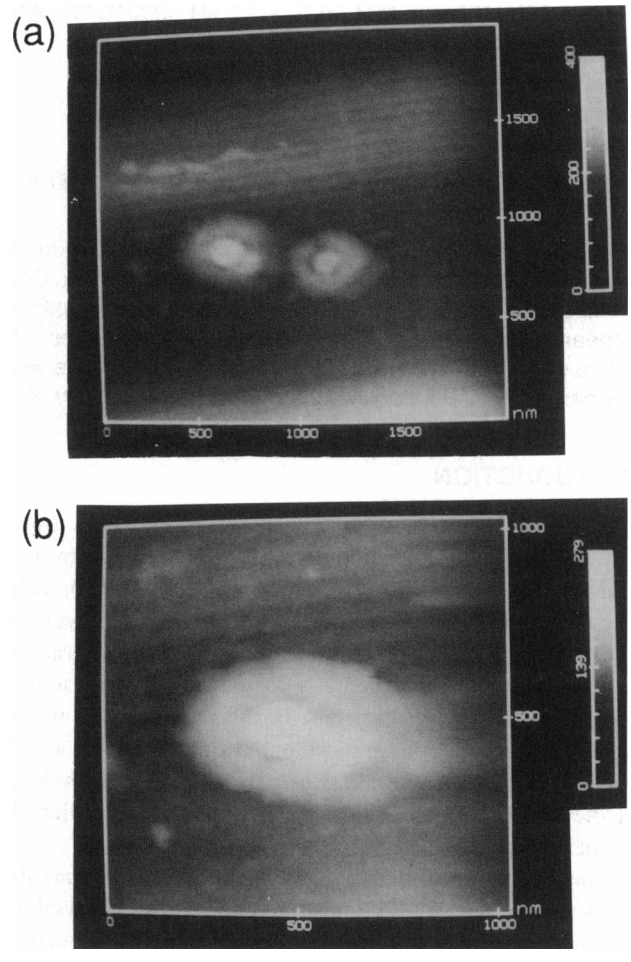

FIGURE 1 AFM images of 90° sections of major ampullate silk strands of *Nephila clavipes*. (*a*) Shows cross sections of two strands. The image size is 2 × 2 μm^2. (*b*) Shows an image of the cross section of another strand. The image size is 1.04 × 1.04 μm^2. The coaxial arrangement of the inner and outer parts of the core can be observed. The small radial gap in the outer core region was observed in most of images of the cross sections of the dry fibers. Its function is at present not known. The stacked double layered structure is due to the pleated fibrillar structure.

RESULTS AND DISCUSSION

90° cross sections

Fig. 1 shows the images of several 90° cross sections of the silk fiber. It is clear that the internal structure of the fiber is highly organized in the radial direction. Two distinct concentric regions separated by a small space could be observed. The inner region seemed to be compact with a possible lobular appearance, whereas the outer region was a ring. In addition, the inner region appeared to be "whiter" than the outer region in the gray-scale representation of the image. This difference in appearance implies different force interactions with the tip or different heights of the two regions. It is tempting to speculate that this difference may be due to the presence of different proteins in the two different regions, as suggested by Lewis (1992). The appearance of the double, stacked layers observed on each of the sections shown in Fig. 1 indicates that the concentric regions were not smooth cylinders but consisted of finer structures that should be observable in sections cut along the fiber axis, as shown below.

45° and longitudinal sections

Fig. 2 illustrates an image obtained on sections of the silk made at 45° to the fiber axis. The two concentric regions observed in Fig. 1 contained pleated structures parallel to the fiber axis. In the image shown, the crests and the bases of the pleats were arranged in an intricate "out-of-phase" fashion in the two regions. It can be deduced that the "layered" appearance of the cross sections of the fibers was due to the inclusion of two or more pleats in the sections. The diameter of the pleated structure in the central region varied along the axis, ranging from 100–300 nm. The individual fibril-like structures making up both regions had an apparent diameter of 100–150 nm. The length of individual pleats on the fibrils varies greatly along the axis of the silk fiber and ranges between 100 and 500 nm. This great irregularity in the periods of the pleats can be observed more clearly in Fig. 3 (*a*), which is an image taken from a longitudinal section through the outer core region of the silk fiber.

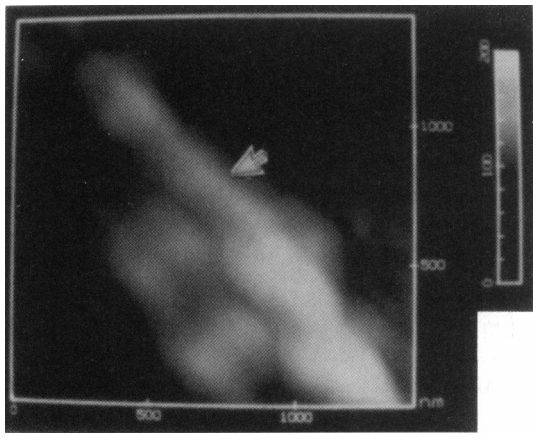

FIGURE 2 AFM images of 45° sections of major ampullate silk strands of *Nephila clavipes*. The image size is 1.4 × 1.4 μm^2. This image shows a conspicuously pleated, fibrillar structure in the center of the core region, which is surrounded by fibrils that have pleats somewhat different in nature. The arrow points to the inner core region. The diameter of the fibrillar structure varies along the axis, and ranges from 100–300 nm. The crests and bases of the pleats in the inner core are out of phase with those in the outer core in this image.

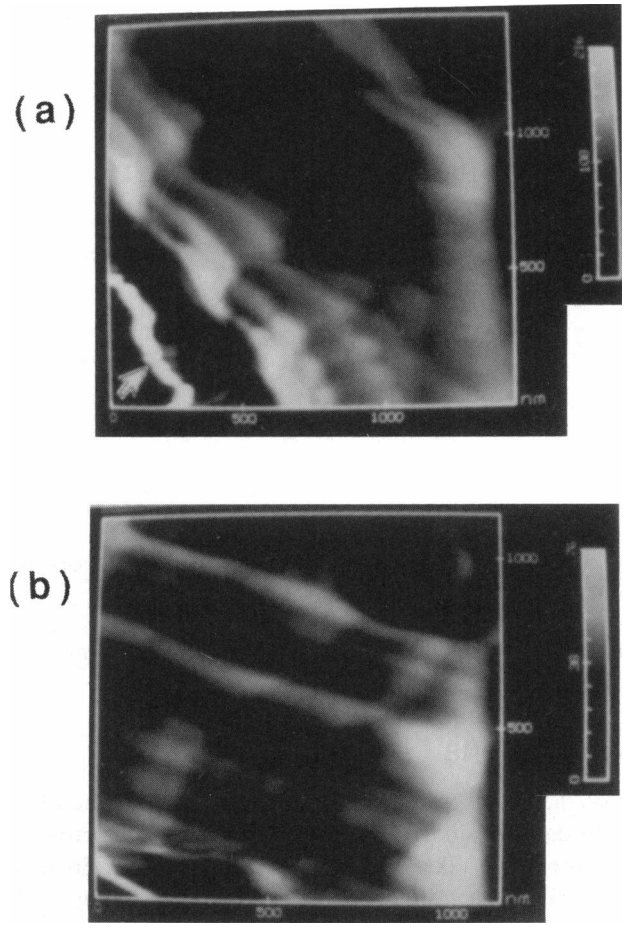

FIGURE 3 AFM images of longitudinal sections of major ampullate silk strands of *Nephila clavipes*. (*a*) Unstretched strand; the image size is 1.5 × 1.5 μm^2. (*b*) Silk stretched to approximately 120% of its original length; the image size is 1.1 × 1.1 μm^2. The depths of the folds in (*a*) are almost an order of magnitude larger than those in (*b*). Also the folds in (*a*) exhibit great irregularity in periods. A skin-core differentiation (the *arrow* points to the skin) can be observed distinctly in (*a*). The diameter of the individual fibrils ranges between 100 and 150 nm. The length of the pleats appears to vary along the axis and is between 100 and 500 nm.

The outstanding mechanical properties of the major ampullate silk is partly due to its breaking extension ratio (BER = length of fiber when maximally extended/original length) of about 1.2–1.4. This ratio and its tensile strength of approximately 1 GPa represent the optimal strength and extension for supporting the maximum static force possible (Denny, 1986). Therefore, we studied the structural characteristics that permit this range of extension by stretching the silk to just below its typical BER. An image of the longitudinal section of the stretched silk is shown in Fig. 3 (*b*). It is apparent that the stretched silk in Fig. 3 (*b*) has a much smoother appearance compared with the distinct pleated patterns exhibited by the unstretched silk in Fig. 3 (*a*). Typical values measured for the depths of the folds in the pleats were between 50 and 60 nm for the unstretched fibers, and between 5 and 20 nm in the case of the stretched fibers. These images suggest a clue to the mechanism that helps spider silk to achieve the optimal BER: the accordion-like pleats extend when the silk is stretched. Whether this mechanism is the only mechanism for elasticity awaits a more detailed study of the correlation of fiber structures with incremental fiber extensions. However, these results do show that any molecular mechanism proposed to explain the BER must take into consideration the formation of the supramolecular pleats.

The images in Fig. 3, (*a*) and (*b*) also show a new structural feature that was not observed in the 45° and 90° sections. Outside of the pleated structures, there seemed to be a thin layer that may be the skin of the silk. Evidence for the existence of a skin in major ampullate silk was described by Work (1984) based on a study made of the viscoelastic behavior of wetted silk fibers (Work, 1985). The ease of fracture between the skin and the core layers was noted and attributed to differences in chemical composition (Work and Young, 1987). However, whether similar skin-core differentiations are present in other types of silks from other species is still an uncertainty (Stubbs et al., 1992; Peters and Kovoor, 1989; Candelas et al., 1986; Nentwig and Heimer, 1987). In the present study, we could observe a skin-like layer in most of our longitudinal sections, although we have not been able to obtain definitive images on the structure of this layer. The fact that we did not observe this layer in the 45° and 90° sections may indicate that this layer could be structurally fragile. Indeed, the skin seemed to have a tendency to separate from the core even in the longitudinal sections. The shearing force of the microtoming knife may cause the separation of the skin and the core layers.

The existence of the highly aligned, quite densely packed fibril-like structure of the core regions of the silk fiber is reminiscent of the fiber structure of Kevlar® (Li et al., 1993), the synthetic fiber with very high modulus and tensile strength. It is reasonable to assume that the strength of the

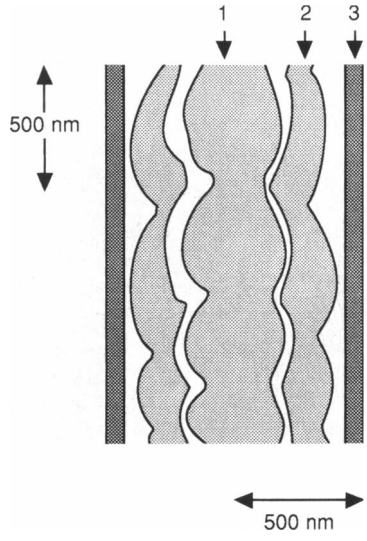

FIGURE 4 Structural model of spider dragline silk. Label 1, inner core region; Label 2, outer core region; Label 3, skin region.

spider silk is also derived from such an ordered arrangement of parallel fibrils.

CONCLUSIONS

From the above results, it is clear that the structure of the spider dragline silk is drastically different from the proposed structure of the silk of silk worm (Gosline et al., 1986; Vollrath, 1992). A new structural model is depicted in Fig. 4. The proposed structure of dragline silk consists of a core (regions 1 and 2 in Fig. 4) and a thin skin (region 3 in Fig. 4). The core further differentiates into the inner (labeled 1) and outer (labeled 2) regions. The outer core surrounds the inner core in a coaxial manner. Both the inner and outer core regions contain pleated fibril-like strands. Furthermore, the inner and outer cores are not identical but may have different protein compositions or different protein structures if only one protein is present. It is interesting to note that in many species of spider, the major ampullate glands exhibit three different secreting regions (Kovoor, 1987), which is consistent with the formation of the three layers in the silk. This model with the highly organized pleated fibrils accounts for both the elastic property and the mechanical strength of dragline silk. The structure-property relations of spider silks that serve other functions will be investigated.

The authors wish to thank Professor R. Lewis for providing the silk and for helpful discussion and S. Fahnestock for critically reading the manuscript. We thank the National University of Singapore for providing partial financial support for S. F. Y. Li.

REFERENCES

Beard, J. 1992. Warding off bullets by a spider's thread, *New Sci.* 136:18.

Binnig, G., C. F. Quate, and Ch. Gerber. 1986. Atomic force microscopy, *Phys. Rev. Lett.* 56:930–933.

Bonthrone, K. M., F. Vollrath, B. K. Hunter, and J. K. M. Sanders. 1992. The elasticity of spiders' webs is due to water-induced mobility at a molecular level. *Proc. R. Soc. B Biol. Sci.* 248:141–144.

Candelas, G. C., A. Ortiz, and C. Molina. 1986. The cylindrical or tubiliform glands of *Nephila clavipes*. *J. Exp. Zool.* 237:281–285.

Denny, M. W. 1986. The physical properties of spider's silk and their role in the design of orb-web. *J. Exp. Biol.* 65:483–506.

Dong, Z., Lewis R. V., and C. R. Middaugh. 1991. Molecular mechanism of spider silk elasticity. *Arch. Biochem. Biophys.* 284:53–57.

Edmonds, D., and F. Vollrath. 1992. The contribution of atmospheric water vapour to the formation, and efficiency of a spider's capture web. *Proc. R. Soc. Lond. B Biol. Sci.* 248:145–148.

Gosline, J. M., M. W. Denny, and M. E. DeMont. 1984. Spider silk as rubber. *Nature (Lond.).* 309:551–552.

Gosline, J. M., M. E. DeMont, and M. W. Denny. 1986. The structure and properties of spider silk. *Endeavour (Oxf.).* 10:37–43.

Hansma, H. G., J. Vesenda, C. Siegerist, G. Kelderman, H. Morrett, R. L. Sinsheimer, V. Elings, C. Bustamante, and P. K. Hansma. 1992. Reproducible imaging and dissection of plasmid DNA under liquid with the atomic force microscope. *Science (Wash. DC).* 256:1180–1184.

Hepburn, H. R., A. D. Chandler, and M. R. Davidoff. 1979. Extensometric properties of insect fibroins: the green lacewing cross-beta, honeybee alpha-helical, and greater waxmoth parallel-beta conformations. *Insect Biochem.* 9:69–77.

Kovoor, J. 1987. Comparative structure and histochemistry of silk- producing organsin Arachnids. *In* Ecophysiology of Spiders. W. Nentwig, editor. Springer-Verlag, Berlin, Heidelberg. 160–186.

Lewis, R. V. 1992. Spider silk - the unravelling of a mystery. *Acc. Chem. Res.* 25:392–398.

Li, S. F. Y., A. J. McGhie, and S. L. Tang. 1993. Internal structure of Kevlar fibers. *Polymer Commun.* 34:4573–4575.

Nentwig, W., and S. Heimer. 1987. Ecological aspects of spider webs. *In* Ecophysiology of Spiders. W. Nentwig, editor. Springer-Verlag, Berlin, Heidelberg. 221–228.

Peters, H. M., and J. Kovoor. 1989. The construction of egg-cases by the spider *Polenecia producta* (Simon, 1873) in relation to the functions of the spinning apparatus. *Zool. Jahrb. Abt. Allg. Zool. Physiol. Tiere.* 93: 125–144.

Rammacher, M., R. W. Tillmann, M. Fritz, and H. E. Gaub. 1992. From molecules to cells: imaging soft samples with the atomic force microscope. *Science (Wash. DC).* 257:1900–1905.

Sanders, J. K. M. 1993. NMR of Nature's plastics and spiders' webs: chemistry, physics, or biology. *Chem. Soc. Rev.* 22:1–7.

Stubbs, G., E. K. Tillinghast, M. A. Townley, and N. A. Cherim. 1992. Fibrous composite structure in a spider silk. *Naturwissenschaften.* 79: 231–234.

Treloar, L. R. G. 1975. Physics of Rubber Elasticity. Oxford Clarendon Press, Oxford, U.K. 310 pp.

Vollrath, F., and D. T. Edmonds. 1989. Modulation of the mechanical properties of spider silk by coating with water. *Nature (Lond.).* 340:305–307.

Vollrath, F., W. J. Fairbrother, R. J. P. Williams, E. K. Tillinghast, D. T. Bernstein, K. S. Gallagher, and M. A. Townley. 1990. Compounds in the droplets of the orb spider's viscid spiral. *Nature (Lond.).* 345:526–528.

Vollrath, F. 1992. Spider webs and silk. *Sci. Am.* 266:70–76.

Work, R. W. 1984. Duality in major ampullate silk and precursive material from orb-web-building spiders (Araneae). *Trans. Am. Microsc. Soc.* 103: 113–121.

Work, R. W. 1985. Viscoelastic behaviour and wet supercontraction of major ampullate silk fibers of certain orb-web-building spiders (Araneae). *J. Exp. Biol.* 118:379–404.

Work, R. W., and C. T. Young, 1987. The amino acid composition of major and minor ampullate silks of certain orb-web-building spiders (*Araneae, Araneidae*). *J. Arachnol.* 15:65–80.

Yang, J, and Z. Shao. 1993. Effect of probe force on the resolution of atomic force microscopy of DNA. *Ultramicroscopy.* 50:157–170.